Appl. Phys. B. 63, 155–159 (1996)

Applied Physics B Lasers and Optics

Optical bistability by nonlinear reflection in a polymeric blend

U. Bernini[1,2], L. De Stefano[2], M. Feo[1,2], P. Mormile[3,*], P. Russo[1,2]

[1] Dipartimento di Scienze Fisiche, Università di Napoli Federico II, Pad. 20 Mostra d'Oltremare, I-80125 Napoli, Italy
[2] Istituto Nazionale per la Fisica della Materia, Unità di Napoli, I-80125 Napoli, Italy
[3] Istituto di Cibernetica, C.N.R., Via Toiano 6, I-80072 Arco Felice, Napoli, Italy
(Fax: + 39-81/5267654, E-mail: MORMILE@serjei.na.cnr.it)

Received: 12 June 1995/Accepted: 30 November 1995

Abstract. We have analysed the propagation of two continuous-wave Ar^+-laser beams travelling in opposite directions in a two-component nonlinear heterogeneous medium (the polymeric blend PMMA-EVA), in a mirror retroreflection geometry. Bistable reflection associated with the laser-induced suppression of scattering is observed. This phenomenon has a thermal origin. Based on light- and heat-transport theory inside the material, a simplified explanation of the experimental evidence is presented, showing the conditions for the onset of optical bistability. Qualitative agreement with our experimental results is found.

PACS: 42.20; 42.70; 61.40

In a previous paper [1], we studied nonlinear scattering in a clear PMMA-based polymer [2, 3] (PMMA-EVA) [Poly-Methyl Methacrylate-poly(Ethylene-co-VinylAcetate), made up by an acrylic matrix (PMMA) and a finely dispersed vinyl rubber (EVA). Using a continuous-wave (CW) laser beam, self-transparency [4] was observed [1] at an intensity threshold as low as 25 W/cm^2. In addition, bistability at a nonlinear interface in PMMA-EVA has been reported [5]. The nonlinear scattering producing such optical phenomena originates from significant thermal nonlinearities in the refractive index of PMMA-EVA (a two-component heterogeneous medium). In fact, the temperature coefficients of the refractive indices (at $\lambda = 514$ nm and $T = 20°C$) are [6]

$$dn_{EVA}/dT = -5.0 \times 10^{-4\circ} C^{-1},$$

$$dn_{PMMA}/dT = -1.2 \times 10^{-4\circ} C^{-1},$$

$$d^2 n_{EVA}/dT^2 = -1.0 \times 10^{-5\circ} C^{-2},$$

$$d^2 n_{PMMA}/dT^2 \approx 0.$$

The difference $\Delta n = n_{PMMA} - n_{EVA}$ between the refractive index of the two blend components is temperature dependent. Previous measurements [1, 6] on the optothermal properties of these materials show that Δn changes its sign around the self-transparency temperature $T_{sf} = 30°C$ (Fig. 1). The trend of dn/dT for PMMA and EVA in the range 20–40°C is shown in Fig. 2.

In such a nonlinear medium, two counter-propagating beams (obtained, e.g., by reflection of the incident beam by a mirror placed at the opposite side of the material slab) may give rise to optical bistability. Such a device (well known as a nonlinear reflector) has already been proposed as one of the simplest means to obtain optical bistability [7].

In this paper, we study the bistable reflection in a slab of the polymeric blend PMMA-EVA.

1 Materials and methods

A plane-parallel disk of the synthetic polymeric blend PolyMethyl-MethAcrylate-poly(Ethylene-co-VinylAcetate) (PMMA-EVA) was analysed (thickness $l = 0.34$ cm, radius $a = 0.32$ cm). The preparation of the PMMA-EVA polymer is reported elsewhere [2]. In order to set the conditions for the observation of optical bistability, we irradiated the disk on one side with a 514 nm cw Ar^+-laser beam. The beam power distribution was Gaussian (measurement of the spatial profile is reported in [1]) and the beam radius on the sample was 7.5×10^{-2} cm. The optical feedback signal (the counter-propagating beam) was obtained by placing a mirror (reflectivity $R = 0.99$) at the opposite side of the slab. The experimental setup is shown in Fig. 3. A Pockels cell, driven by a sawtooth-wave generator (frequency = 10^{-3} Hz), is used to slowly vary the incident laser intensity linearly in the range 0–24 W/cm^2. Such a slow scan of the intensity range (duration of the scan from zero up to the maximum incident power was 1000 s) is required in order to allow the laser-irradiated sample to be in thermodynamical equilibrium at each input power level. Indeed, we have evidence that the hysteresis phenomenon reported here

* To whom all correspondence should be addressed

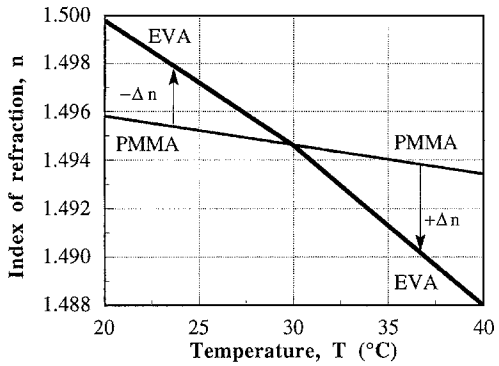

Fig. 1. Refractive index (at $\lambda = 514$ nm) of the polymer PMMA and co-polymer EVA as a function of temperature. The plot shows the linear (for PMMA) and quadratic (for EVA) trend of the refractive index deduced from the measured values reported in [1]

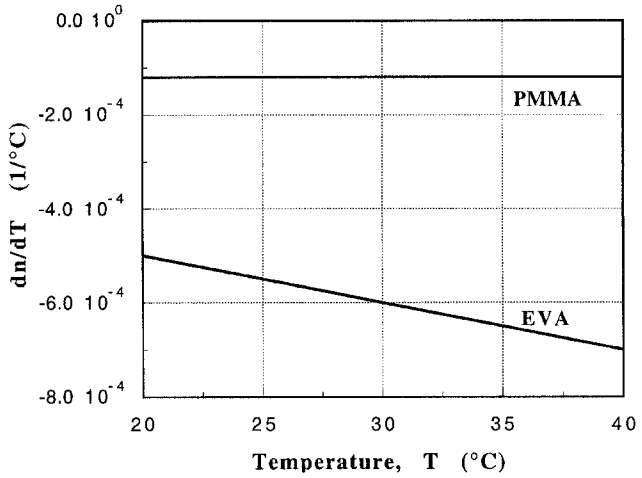

Fig. 2. Temperature coefficient of the refractive index of PMMA and EVA as a function of temperature measured at $\lambda = 514$ nm. This plot is the linear trend from the measured values of the first- and second-order temperature derivatives of the refractive index (deduced from [6])

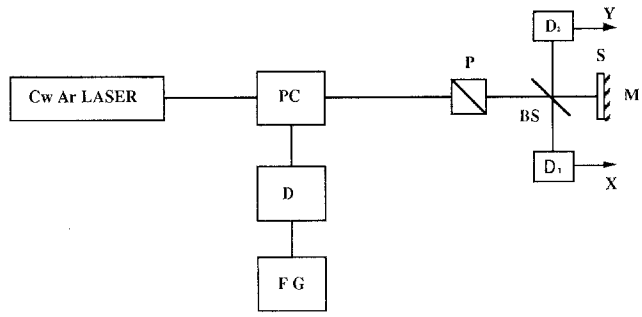

Fig. 3. Experimental arrangement for counter-propagating beams in the sample (*PC* Pockels cell; *D* Driver; *FG* Function generator; *P* Polarizer; *BS* Beam splitter; *S* Sample; *M* Mirror; D_1, D_2 Photodiodes; *X*, *Y*: Signals to the data-acquisition system)

(Sect. 3) can be repeatedly observed with the same features when the duration of the scan is several hundreds of seconds or higher.

The incident light intensity on the sample and the output light from the disk after passing the sample twice are collected by photodiodes D_1 and D_2, respectively. A data-acquisition system is utilised to store the experimental data digitally and to provide the X–Y signals for an analog recorder.

2 Theory

The propagation of a collimated beam normally incident on a plane-parallel scattering medium can be studied qualitatively using the four-fluxes transport theory [8,9]. In this work, we consider the case of two oppositely travelling collimated beams inside the medium, a forward beam and a backward beam generated by using a mirror at the rear side of the disk. By supposing that the incident intensity is high enough that the diffused fluxes can be neglected, we may take into account only the forward and backward collimated fluxes I^+ and I^-, respectively. As function of the depth z inside the medium, $I^+(z)$ and $I^-(z)$ are provided by solving the coupled equations

$$\frac{dI^+}{dz} = -(\alpha + \beta^+ + \beta^-)I^+,$$

$$\frac{dI^-}{dz} = (\alpha + \beta^+ + \beta^-)I^-, \tag{1}$$

with the boundary conditions

$$I^+(z)|_{z=0} = I_0^+,$$

$$I^-(z)|_{z=l} = RI^+(r)|_{z=l},$$

where R is the reflectivity of the mirror, α the absorption coefficient of the medium, and β^+ and β^- are the scattering coefficients from a collimated beam into a diffused flux in the positive z-direction and in the negative one, respectively. In the two-component heterogeneous medium PMMA-EVA, the scattering is determined by the difference Δn between the refractive indices n_{PMMA} and n_{EVA} of the two components: $\Delta n = n_{\text{PMMA}} - n_{\text{EVA}}$; Δn has both a linear and a nonlinear term. In the limit of weak scattering, the scattering coefficients β^+ and β^- are proportional to $(\Delta n)^2$:

$$\beta^+ = k^+(\Delta n)^2, \quad \beta^- = k^-(\Delta n)^2, \tag{2}$$

where the parameters k^+ and k^- depend on the dimensions, shape and concentration of the scattering particles and on the wavelength of light.

In a medium with losses of thermal origin, we have $\Delta n = \Delta n(T)$, where T is the temperature of the sample. By irradiating the sample with a cw laser beam, a temperature rise $\Delta T = T - T_0$ above the room temperature T_0 is induced in the material. By power-series expansion around T_0 to second order in ΔT, we can write

$$\Delta n(T) \cong \Delta n(T_0) + A(\Delta T) + B(\Delta T)^2, \tag{3}$$

where the coefficients A and B are given by

$$A \equiv \left(\frac{\mathrm{d}(\Delta n)}{\mathrm{d}T}\right)_{T=T_0} = \left(\frac{\mathrm{d}n_{\mathrm{PMMA}}}{\mathrm{d}T}\right)_{T=T_0} - \left(\frac{\mathrm{d}n_{\mathrm{EVA}}}{\mathrm{d}T}\right)_{T=T_0}, \quad (4)$$

$$B \equiv \frac{1}{2}\left(\frac{\mathrm{d}^2(\Delta n)}{\mathrm{d}T^2}\right)_{T=T_0} = \frac{1}{2}\left(\frac{\mathrm{d}^2 n_{\mathrm{PMMA}}}{\mathrm{d}T^2}\right)_{T=T_0} - \frac{1}{2}\left(\frac{\mathrm{d}^2 n_{\mathrm{EVA}}}{\mathrm{d}T^2}\right)_{T=T_0}. \quad (5)$$

By introducing approximation (3) and (2), the system (1) can be written as

$$\frac{\mathrm{d}I^+}{\mathrm{d}z} = -[\alpha + \beta(T)]I^+,$$

$$\frac{\mathrm{d}I^-}{\mathrm{d}z} = [\alpha + \beta(T)]I^-, \quad (6)$$

where

$$\beta(T) \equiv (k^+ + k^-)[\Delta n(T)]^2 = \beta(T_0)\left(\eta + \frac{|A\Delta T + B(\Delta T)^2|}{|\Delta n(T_0)|}\right)^2. \quad (7)$$

$$\eta = \mathrm{sign}\,\{\Delta n(T_0)[A\Delta T + B(\Delta T)^2]\} = \pm 1,$$

and

$$\beta(T_0) = (k^+ + k^-)[\Delta n(T_0)]^2$$

is the linear scattering coefficient.

If a temperature rise ΔT is induced in the sample by cw laser irradiation, then $\Delta T = \Delta T(I)$, where I is the light intensity in the medium ($I = I^+ + I^-$); one has for the difference Δn between the refractive indices of the two components of the medium $\Delta n = \Delta n(I)$. Hence, from (7), we can see that for $\eta = -1$ a nonlinear clearing appears as I approaches a critical value I_{sf}, so that

$$\frac{|A\Delta T(I_{\mathrm{sf}}) + B(\Delta T)^2\ (I_{\mathrm{sf}})}{|\Delta n(T_0)|} = 1.$$

At first order, if α is neglected in (6), it can be demonstrated [7] that when the self-transparency condition $\eta = -1$ is met, the output beam intensity $I^-(z=0)$ as a function of the incident beam intensity $I^+(z=0)$, can be multivalued. For a theory of such nonlinear phenomena, we have to add a description of the heat transport to (6) for light transport in the irradiated material. The general steady-state heat transfer equation in cylindrical coordinates is

$$K\frac{\partial^2 T}{\partial z^2} + \frac{K}{r}\frac{\partial}{\partial r}\left(r\frac{\partial T}{\partial r}\right) = -\alpha(I^+ + I^-), \quad (8)$$

where K is the thermal conductivity of the sample. In order to obtain a simplified but realistic description of the problem, we introduce some approximations. In (6), the transverse intensity is neglected. If we consider only the axial (z-coordinate) heat transport in the sample, i.e., we neglect the transverse temperature gradients along the radial coordinate r, the coupled light–heat-transport equations reduce to unidimensional ordinary equations that can be solved numerically for given initial conditions, yielding the axial temperature profile $T(z)$ in the sample (for a given incident intensity), the local value of the scattering coefficient $\beta(T)$ as a function of z, and, finally, $I^+(z)$ and $I^-(z)$. However, this approximation holds for a uniformly illuminated laterally infinite disk ($a = \infty$). If the beam has a Gaussian power distribution $I = I(r)\exp(-r^2/w^2)$, where w is the beam radius with $w < a$, the transverse heat flux in the sample along the radial coordinate r must be taken into account, whereby $T = T(r, z)$ and $I = I(r, z)$. The occurrence of lateral scattering broadens both the temperature and the radial intensity profile. Then, in order to obtain a simplified description of the temperature distribution, we used a quasi-unidimensional heat equation derived from (8) by averaging the temperature and light fields over the beam cross section. The transverse heat flow was taken into account by introducing an effective heat exchange coefficient K', so that the heat equation reduces to

$$K\frac{\mathrm{d}^2 T}{\mathrm{d}z^2} - K'(T - T_0) = -\alpha(\langle I^+\rangle + \langle I^-\rangle), \quad (9)$$

where $\langle I^+\rangle$ and $\langle I^-\rangle$ are the average values of the intensities over the beam cross section. The coupled set of eqs. (6) (with $I \equiv \langle I\rangle$) and (9) have been solved numerically for our experimental conditions, with the constant K' and the boundary conditions determined as explained in the appendix.

3 Results

In Fig. 4, the reflected intensity $I^-(z=0)$ is plotted as a function of the incident intensity $I^+(z=0)$ for three values of the linear scattering coefficient $\beta(T_0) = 5,\ 7,\ 10\ \mathrm{cm}^{-1}$ at room temperature $T_0 = 20°\mathrm{C}$, as provided by the solution of (6) and (9) in Sect. 2. At $T_0 = 20°\mathrm{C}$, in (7), $\eta = -1$. In fact, the quantities A and B defined in (4) and (5) are positive at this temperature, $\Delta n(T_0)$ is negative (Fig. 1). Figure 4 indicates that at a threshold value $\beta(20°\mathrm{C}) \cong 7\ \mathrm{cm}^{-1}$, the incident light shows bistable reflection. We point out that the boundary conditions have no effect on the threshold value of β for optical bistability. On the contrary, they affect the value of the incident intensity $I^+(z=0)$ at which the bistability turning point occurs. The bistable behaviour disappears when $\eta = +1$ in (7). For PMMA-EVA, this occurs for $T_0 > 30°\mathrm{C}$ where $\Delta n(T_0) > 0$ (Fig. 1), A and B are again positive quantities at these temperatures.

Figure 5 shows the experimental data for the relationship between input and output intensities (i.e., I^- vs I^+ at $z=0$) upon laser irradiation of the PMMA-EVA slab at $T_0 = 20°\mathrm{C}$. In our experimental conditions, the linear scattering coefficient obtained from measurements of collimated transmittance [1] was $\beta(T_0) = 1.2\ \mathrm{cm}^{-1}$. In the forward path, the output intensity increases nonlinearly with increasing input intensity. At the maximum intensity scanned ($I^+ = 24\ \mathrm{W/cm}^2$), a decrease of the input intensity produces an inversion in the curve, but along

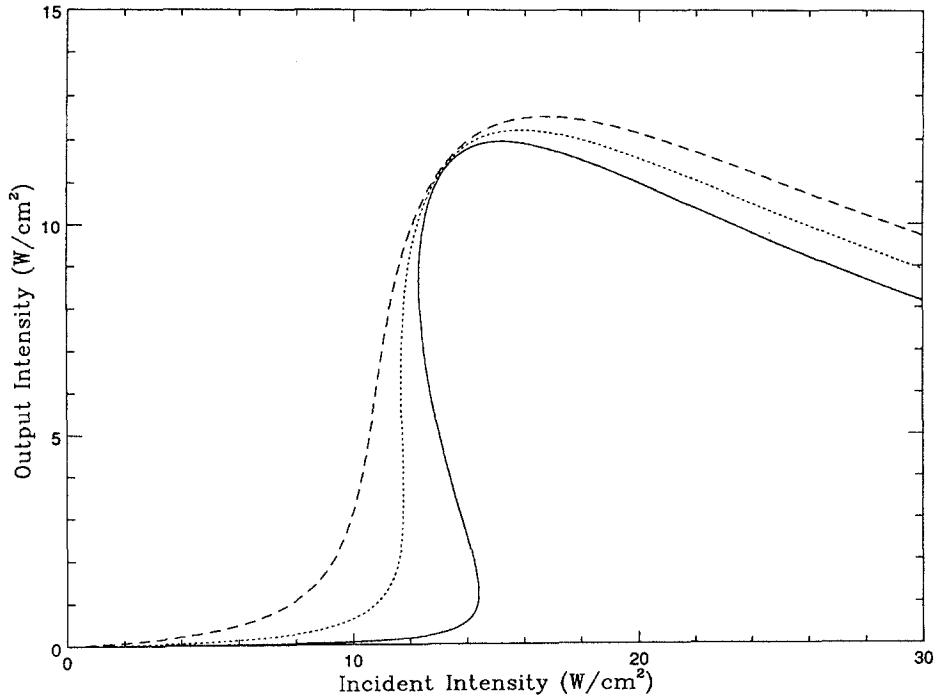

Fig. 4. Reflected intensity $I^-(z=0)$ at the front surface of the nonlinear reflector as a function of the incident intensity $I^+(z=0)$, calculated by solving (6) and (9) numerically for a slab of PMMA-EVA. Temperature $T_0 = 20°C$ (*Solid curve*: $\beta(T_0) = 10\ \mathrm{cm}^{-1}$; *dotted curved*: $\beta(T_0) = 7\ \mathrm{cm}^{-1}$, *dashed curve*: $\beta(T_0) = 5\ \mathrm{cm}^{-1}$)

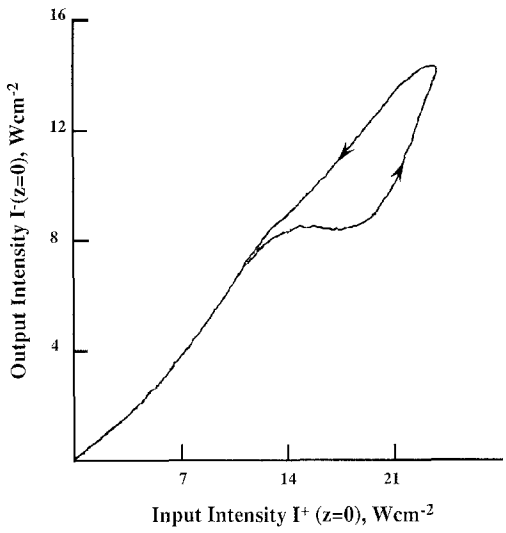

Fig. 5. Experimental evidence of optical bistability in PMMA-EVA. The output intensity is plotted as a function of the input intensity. This plot is produced by the X–Y analog recorder (Sect. 1). The *arrows* indicate the direction of the forward and backward scan of the incident intensity. A hysteresis loop appears at about 12 W/cm²

a different path than the forward one: a hysteresis cycle appears, whose loop closes at the inflection point ($I^+ = 12\ \mathrm{W/cm^2}$). The hysteresis phenomenon observed in the retroreflection geometry for a slab of the polymer PMMA-EVA, as shown in Fig. 5, indicates experimentally the existence of a bistable behaviour. We observed this phenomenon by slowly scanning the incident intensity in the range 0–24 W/cm² at a rate of 24×10^{-3} W/cm² s but it was confirmed in another series of measurements (not shown here for brevity) in which we changed I^+ step-by-step at a rate of about 4 min per data point.

4 Discussion

The bistability phenomenon shown experimentally in Fig. 5, and predicted theoretically in Fig. 4, is of thermal origin and can be related to other typical nonlinear optical phenomena already observed in this polymeric blend in our previous studies [1, 5]. In order to explain the experimental results reported here, we have used an approximate steady-state solution of the coupled heat- and light-transport equations inside PMMA-EVA. This theory shows that bistable reflection does occur for the range of input intensity used in our experiments, but for a value of the linear scattering coefficient ($\beta \geq 7\ \mathrm{cm}^{-1}$) much higher than the one predicted for our sample ($\beta = 1.2\ \mathrm{cm}^{-1}$). In other words, the theory predicts bistability for a significantly optically thicker sample. The quantitative disagreement could be ascribed to the approximation introduced in the solution of the transport equations, or more likely, to the inadequacy of (1), used to describe the scattering in PMMA-EVA. These equations can be exactly utilised only if we neglect the diffused radiation completely, which, on the contrary, can play a role in our situation. In fact, transmission electron micrographs show that for the typical linear dimension $2r$ of EVA inclusions in PMMA, the value of the scattering parameter is $2\pi r/\lambda \gg 1$. Nevertheless, since $n_{\mathrm{EVA}} \cong n_{\mathrm{PMMA}}$, $2\pi|\Delta n|/\lambda_0 \ll 1$, where λ_0 is the wavelength of the light in free space. This implies that the scattering is of the Rayleigh-Gans type with a cross section $\sigma_S \propto |\Delta n|^2$ and is highly anisotropic (forward peaked). The anisotropy of the scattering implies that part of the radiation is diffused in the propagation direction of the collimated beam (the scattering is mostly concentrated in a forward angular region), while the four-fluxes theory used here essentially predicts that the diffused fluxes cannot be converted into

collimated fluxes. However, our simplified theory avoids the great complexity of introducing the diffused radiation into (1) while giving good qualitative agreement with experiments.

The striking nonlinear optical properties exhibited by this solid material are certainly of interest for nonlinear reflecting devices.

Appendix

Equation (8) can be solved with the following boundary conditions:

$$K\left.\frac{\partial T}{\partial z}\right|_{z=0} = H(T_{z=0} - T_0), \tag{A1}$$

$$K\left.\frac{\partial T}{\partial z}\right|_{z=l} = -H(T_{z=l} - T_0), \tag{A2}$$

$$\left.\left(\frac{\partial T}{\partial r}\right)\right|_{r=0} = 0, \tag{A3}$$

$$K\left.\frac{\partial T}{\partial r}\right|_{r=a} = -H(T_{r=a} - T_0), \tag{A4}$$

where a and l are the radius and the thickness of the considered cylindrical sample, respectively, and H is the coefficient of surface heat transfer between sample and air.

In our theoretical approach, we assumed the same approximations in order to describe the temperature field in a simple way. Starting from (8) and averaging over the beam cross section of radius w, we obtain

$$K\frac{\partial^2 T}{\partial z^2} + \frac{2K}{w}\left(\frac{\partial T}{\partial r}\right)_{r=w} = -\alpha(\langle I^+\rangle + \langle I^-\rangle). \tag{A5}$$

By neglecting any heat generation for $r > w$, the temperature profile can be assumed to have the following radial dependence:

$$T(r) = C\ln(a/r) + T_{r=a}, \quad r \geq w,$$

where C is a constant. From the continuity conditions at $r = w$, for T and $\partial T/\partial r$, and using (A4), (A5) becomes

$$K\frac{\mathrm{d}^2 T}{\mathrm{d}z^2} - K'(T_{r=w} - T_0) = -\alpha(\langle I^+\rangle + \langle I^-\rangle), \tag{A6}$$

with

$$K' = \frac{2Ha/w^2}{1 + \frac{aH}{K}\ln(a/w)}. \tag{A7}$$

By setting $T = T_{r=w}$ for $r \leq w$, we obtain (9).

The numerical solution of the coupled equations (6–9) with the boundary conditions (A1), (A2) and the further conditions

$$I^+(z)|_{z=0} = I_0^+, \quad I^-(z)|_{z=l} = RI^+(z)|_{z=l}, \tag{A8}$$

where R is the reflectivity of the mirror, allows for the derivation of the reflected intensity I^- as a function of the incident intensity I^+. The system (6–9) has been solved for a PMMA-EVA disk with dimensions $l = 0.34$ cm and $a = 0.32$ cm, and $w = 7.5 \times 10^{-2}$ cm. We estimated for this material $K \cong 2 \times 10^{-3}$ W/cm °C and $H = 0.6 \times 10^{-2}$ W/cm^2 °C [1]. The parameters A and B depend on the properties of the components and on the temperature T_0. In our case (at $\lambda = 514$ nm and $T_0 = 20$ °C), A and B are positive quantities: $A = +3.8 \times 10^{-4}$°C^{-1}, and $B = +0.5 \times 10^{-5}$°C^{-2} (Fig. 2). The absorption coefficient α can be considered as constant: $\alpha \cong 0.2$ cm^{-1} [3]. In fact, both of the components have approximately the same absorption coefficient at $\lambda = 514$ nm. The only parameters depending on the structure of the blend are k^+ and k^- which determine the linear scattering coefficients β^+ and β^-. At the same concentration, different values of β^+ and β^- can be obtained by varying the dimensions of the scattering particles.

Acknowledgements. The authors wish to thank Mr. E. Casale and Mr. S. Piscitelli for their technical assistance.

References

1. U. Bernini, L. De Stefano, P. Mormile, P. Russo: Opt. Commun. **112**, 169 (1994)
2. P. Laurienzo, M. Malinconico, G. Ragosta, M.G. Volpe: Angew. Makromol. Chem. **170**, 137 (1989)
3. U. Bernini, G. Carbonara, M. Malinconico, P. Mormile, P. Russo, M.G. Volpe: Appl. Opt. **31**, 5794 (1992)
4. G.B. Al'tshuler, V.S. Ermolaev, K.I. Krylov, A.A. Manenkov, A.M. Prokhovar: J. Opt. Soc. Am. B **3**, 660 (1986)
5. U. Bernini, L. De Stefano, P. Mormile, G. Pierattini, P. Russo: Appl. Phys. B **57**, 199 (1993)
6. U. Bernini, M. Malinconico, E. Martuscelli, P. Mormile, P. Russo, M.G. Volpe: J. Mater. Sci. **28**, 6399 (1993)
7. G.B. Al'tshuler, M.V. Inochkin, A.A. Manenkov: Sov. Phys. Dokl. **30**, 574 (1985)
8. N.C. Kothari: J. Opt. Soc. Am. B **5**, 2348 (1988)
9. N.C. Kothari, C. Flytzanis: Opt. Lett. **12**, 492 (1987)